Int J Clin Exp Med 2019;12(1):371-377
www.ijcem.com /ISSN:1940-5901/IJCEM0082325

Original Article

Apoptosis of human hepatocellular carcinoma cells SMMC-7721 induced by C-3 methylidene thiazolidinedione acetic acid

Hong-Xia Liang[1], Yi-Hua Yu[1], Xiao-Hua Li[1], Nai-Fu Tang[1], Guo-Qiang Hu[2], Bin Liu[1]

[1]Institute of Nursing and Health, Henan University, Kaifeng, Henan, China; [2]College of Pharmacy, Henan University, Kaifeng, Henan, China

Received July 9, 2018; Accepted September 12, 2018; Epub January 15, 2019; Published January 30, 2019

Abstract: *Objective:* The objective of this study was to investigate the effect of rufloxacin derivative C-3 methylidene thiazolidinedione acetic acid on apoptosis of human hepatocellular carcinoma cells SMMC-7721. *Methods:* Human hepatocellular carcinoma cells SMMC-7721, esophageal cancer cells EC-9706, colon cancer CaCO-2 cells, and hepatocytes L-02 were cultured i*n vitro* with various concentrations of 6-fluoro -7-(4-methylpiperazin-1-yl)-8, 1-(sulfolatosyl)-1,4-dihydro-4-oxo-3-(3-carboxymethyl-2, 4-thiazolidinedione- 5-methylidene) quinoline (R16). MTT assay was used to detect the inhibitory effect of R16 on proliferation in all cell lines. DAPI fluorescent staining and TUNEL assay were used to detect the changes of apoptosis. PI staining and flow cytometry were used to detect cell cycle changes. p53 and caspase-3 protein expression levels were detected by Western blot. *Results:* R16 significantly inhibited cell proliferation of SMMC-7721, EC-9706 and CaCO-2 cells under the concentration of 2-20 μmol·L^{-1}. The 24 hour IC_{50} values were 3.912, 4.215 and 3.380 mol·L^{-1}, respectively. The 24 hour IC_{50} value of L-02 cells was 35.224 μmol·L^{-1}. The 24 hour IC_{50} value of rufloxacin was 226.924 μmol·L^{-1} for SMMC-7721. The 24 hour IC_{50} value of sunitinib was 7.846 μmol·L^{-1} for SMMC-7721. Following R16 treatment, cell cycle of SMMC-7721 was arrested at G_1-S phase and the apoptosis rate was significantly higher compared to the control group ($P<0.05$). R16 significantly increased p53 and caspase-3 expression in SMMC-7721 cells. In addition, the active fragment of caspase-3 was significantly increased. *Conclusions:* Rufloxacin-rhodanine derivatives exhibited a selective inhibitory effect on cancer cells and significantly induced apoptosis of human hepatocellular carcinoma cells SMMC-7721.

Keywords: Rufloxacin-Rhodanine derivatives, hepatocellular carcinoma cells, cell proliferation, apoptosis, cell cycle

Introduction

Quinolones are widely used as anti-infective agents in clinical practice [1]. This type of agents are inhibitors of DNA gyrase, a type II DNA topoisomerase [2]. The acting mechanism of this enzyme is to perform DNA strands cleavage, change DNA topological structures and reconnect the structures. The enzyme plays an important role in DNA replication, transcription and repair [3]. In eukaryotic cells, some sequence fragments of topoisomerase II have a high degree of homology with DNA gyrase [4]. Some of the fluoroquinolones carboxylic acids commonly used in clinical application, such as ciprofloxacin, rufloxacin, and ofloxacin, have a mild inhibitory effect on eukaryotic topoisomerase II activity [5]. Therefore, quinolone antibiotics with effective structure modifications are expected to become a novel class of anti-cancer candidate compounds. It has been reported that following structure modifications, most anti-cancer fluoroquinolone compounds are topoisomerase II toxins and able to kill tumor cells by stabilizing topoisomerase II mediated cleavable complex to block the connection of DNA double strands, similar to the role of doxorubicin in clinical application [6]. The mechanism of action is mainly associated with inhibition of DNA topoisomerase II activity and induction of apoptosis [7, 8]. In the beginning the modification on anti-bacterial fluoroquinolones was focused on the structure modification on N-1 and C-7 of quinoline ring, and polycyclic quinolone derivatives with anti-cancer

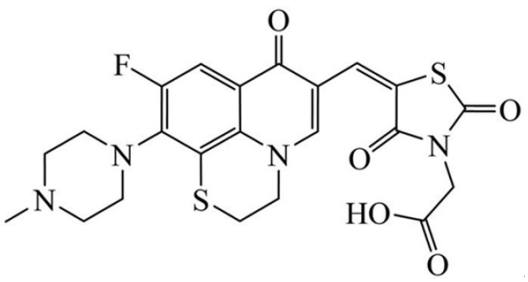

Figure 1. Structure of 6-fluoro-7-(4-methylpiperazin-1-yl)-8,1-(thioethylene)-1,4-dihydro-4-oxo-3-[5-(3-carboxymethyl-2,4-thiazolidinedione) ylidene]-quinoline.

activity were synthesized. However, these compounds failed prior to clinical evaluation due to their in vivo toxicity, low bioavailability and inability to be metabolized [9]. The carboxyl group on C-3 of fluoroquinolone carboxylic acid is required for anti-bacterial activity but has no effect on anti-cancer activity [10]. The five-membered azole heterocyclic ring has been used as a backbone with dominant pharmacophores in the design of drug molecules, among which thiazolidinediones have gained a lot of attention due to their pharmacological activities. Based on the research of fluoroquinolone C-3 rhodanine unsaturated ketones, according to isosteres and splicing principles, thiazolidinedione was used, instead of thio-thiazolidinedione, as the isostere of fluoroquinolones C-3 carboxyl group. A series of fluoroquinolone derivatives were designed and synthesized with good solubility, low molecular weight, unsaturated ketone structures and similar structures to of chalcones and tyrosine kinase inhibitor sunitinib. The anti-tumor activity of this type of compounds was screened. The results showed that this type of derivatives all had good anti-tumor activity. Among these compounds, 6-fluoro-7-(4-methylpiperazin-1-yl)-8, 1-(sulfolatosyl)-1,4-dihydro-4-oxo-3-(3-carboxymethyl-2,4-thiazolidinedione-5-methylidene) quinoline (R16) exhibited the strongest activity, with an IC_{50} up to 3.912 μmol/L and further research and development value (**Figure 1**).

Materials and methods

Main reagents and instruments

Inducer: Rufloxacin derivative C-3 methylidene thiazolidinedione acetic acid was designed and synthesized by the Institute of Chemical Biology of Henan University. The agent was dissolved in dimethyl sulfoxide (DMSO, Solarbio Co.) at a beginning concentration of 1×10^{-2} mol·L^{-1}.

Cell lines and major reagents

Human hepatocellular carcinoma cells SMMC-7721 and human esophageal cancer cells EC-9706 were cultured in DMEM media (Gibco) containing fetal bovine serum (Hangzhou Four Seasons Bioengineering Material Inc.) at a concentration of 0.1% (v/v). Colon cancer CaCO-2 cells and hepatocytes L-02 were cultured in RPMI -1640 media (Gibco) containing fetal bovine serum at a concentration of 0.1% (v/v). Cells were placed in an incubator with 0.05% (v/v) CO_2 at 37°C. Tetramethyl azolium salt (mTT) was purchased from Solarbio Co. DAPI was purchased from Sigma. DeadEnd™ Fluorometric TUNEL System was purchased from Promega. Mouse monoclonal anti-casepase-3 antibody was purchased from Novus. Rabbit polyclonal anti-p53 antibody was purchased from Baiqi Co. Mouse anti-β-actin polyclonal antibody was purchased from Zhongshan Jinqiao Co. HRP-labeled goat anti-rabbit and goat anti-mouse antibodies were purchased from Santa Cruz Co. The remaining reagents were domestic analytical reagents.

Major equipment

The CO_2 incubator (Forma 3121) and plate reader (Multiskan Ascent) were purchased from Thermo. The inverted microscope was purchased from Leica Microsystems. BX51 fluorescent microscope was provided by Olympus. High speed centrifuge was purchased from Eppendorf. Gel imaging system was purchased from UVP, LLC. Flow cytometer was provided by AceaBio Co. Electrophoresis and semi-dry blotting membrane transfer system were purchased from Six-One Electronic Equipment Manufacturing.

Methods

Effects of drugs on cell proliferation by MTT assay: Cells were inoculated on a 96-well plate at a concentration of 16×10^{7}·L^{-1}. Various concentrations of R16 was added to the culture and the media was removed after 24, 48, 72 hour treatment. 0.15 ml DMSO was added to each well. The plate was shaken for 8 minutes and the absorbance at 570 nm was detected in

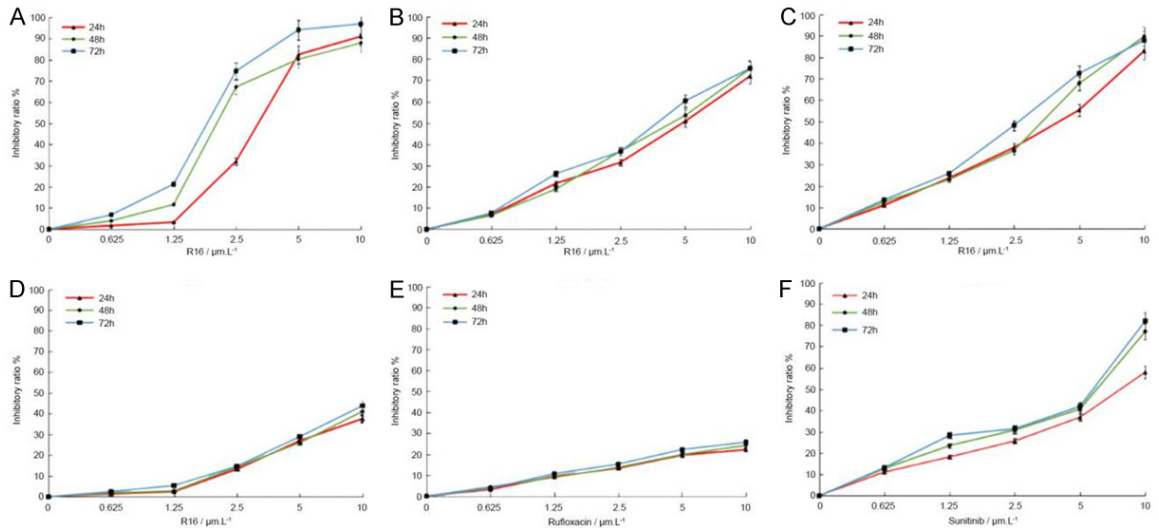

Figure 2. Proliferation inhibition effect of R16, Rufloxacin, and Sunitinib on human cancer cells and L-02 cells. SMMC-7721 cells (A), EC-9706 cells (B), CaCO-2 cells (C) and L-02 (D) cells were treated with various concentration of R16 for 24-72 hours. SMMC-7721 cells were treated with various concentration of Rufloxacin (E) and Sunitinib (F) for 24-72 hours.

a plate reader. The absorbance of wells containing no cells but the same volume of culture media and DMSO was used as control.

Cell Growth Inhibition Rate = [1-(OD value of treated group - OD value of control group)/(OD value of untreated group - OD value of control group)] × 100%.

Observation of cell morphological changes by DAPI staining

Cells were inoculated at a concentration of 4 × $10^7 \cdot L^{-1}$ in the 6-well plate where cover slides were placed at the bottom of wells. After cell adhesion, various concentrations of R16 was added and cultured for 24 hours. Cells were washed twice by PBS and fixed in paraformaldehyde for 20 minutes. 20 μl DAPI working solution was added on the cover slides. After 10 minute staining at room temperature, slides were washed three times by PBS, blocked by 78% neutral glycerol, and observed under the fluorescent microscope.

The apoptosis rate determined by TUNEL assay

Cells were inoculated at a concentration of 4 × $10^7 \cdot L^{-1}$ in the 6-well plate where cover slides were placed at the bottom of wells. Various concentrations of R16 was added and cultured for 24 hours. TUNEL assay was performed following the kit instruction from Promega and the apoptosis rate was calculated.

Observation of cell cycle flow cytometry with PI staining

Cells were inoculated in a cell flask at a concentration of 1 × $10^9 \cdot L^{-1}$ and cultured for 12 hours. Various concentrations of R16 was added and cultured for 24 hours. Cells were collected into an EP tube, washed once by PBS, fixed by 70% ethanol, washed by PBS once and stained by PI for 30 minutes in the dark at room temperature. Cells were detected by flow cytometry.

Detection of protein expression by western blot

Cells were treated by various concentrations of R16 for 24 hours. 200 μL RIPA lysis buffer was added to thoroughly lyse cells. Cells were centrifuged at 4°C (12000 $r \cdot min^{-1}$) for 5 minutes for protein extraction. Protein concentration was detected by Coomassie blue and G250 spectrophotometer. Protein samples were subjected to 12% SDS-PAGE and transferred to PVDF membrane. The membrane was blocked in 5% fat free milk for 1 hour, incubated overnight with the primary antibody at 4°C and then with the secondary antibody for 1 h. Results were shown by chemiluminescence and analyzed by gel imaging system.

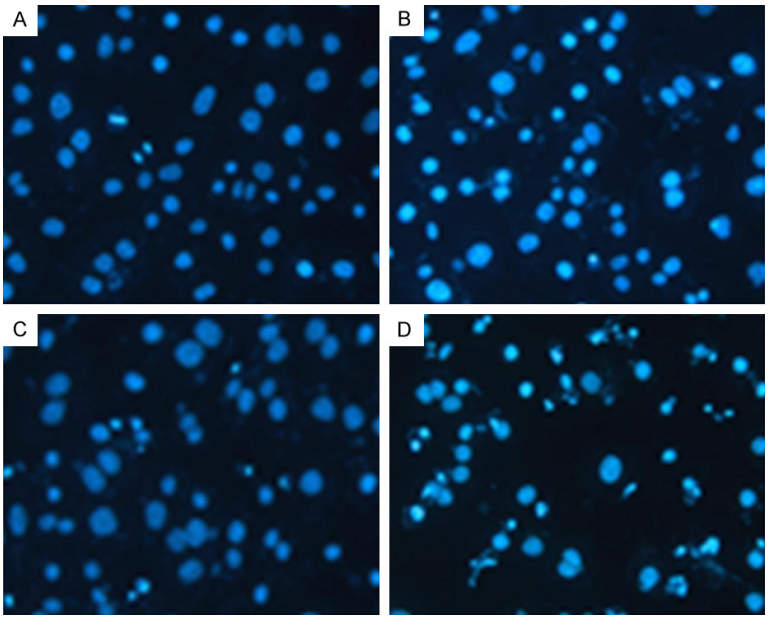

Figure 3. SMMC-7721 cells apoptosis under fluorescent microscope stained by DAPI (× 200). A: Control; B: R16 (2.543 μmol·L^{-1}); C: R16 (3.912 μmol·L^{-1}); D: R16 (5.427 μmol·L^{-1}).

Statistical analysis

Data were analyzed by EXCEK and SPSS 17.0 software. Quantitative data are expressed using $\bar{x} \pm s$. Comparisons between groups were analyzed by t-test.

Results

Inhibition of proliferation of various types of cells by R16

SMMC-7721, EC-9706, and CaCO-2 cells were treated by various concentrations of R16 for 24, 48, and 72 hours, respectively. R16 exhibited a substantial inhibitory effect on proliferation of cancer cells in a time and concentration dependent manner. The IC_{50} values for 24 hour treatment were 3.912 μmol·L^{-1} (r^2=0.8293), 4.215 μmol·L^{-1} (r^2=0.8926) and 3.380 μmol·L^{-1} (r^2=0.9568), respectively. L-02 cells were treated by R16 for 24, 48, and 72 hours, and failed to show significant inhibitory effect on cell proliferation. The IC_{50} value for 24 hour treatment was 35.224 μmol·L^{-1} (r^2=0.9287). The synthetic raw material of R16, rufloxacin had no significant inhibitory effect on SMMC-7721 proliferation, with a 24 hour IC_{50} of 226.924 μmol·L^{-1} (r^2=0.7981). Sunitinib significantly inhibited SMMC-7731 proliferation, with a IC_{50} value of 24 hour treatment of 7.46 μmol·L^{-1} (r^2=0.9650), significantly higher than that of R16 on SMMC-7721 cells (**Figure 2**).

Induction of SMMC-7721 apoptosis by R16

The results of DAPI staining showed that after 24 hour treatment of R16, SMMC-7721 cells exhibited apoptotic morphological changes, including nuclear fragmentation and dissolution, and chromatin condensation, shrinkage, and marginalization (**Figure 3**). TUNEL assay results showed that with an increasing concentration of R16, apoptotic cells were significantly increased in a concentration dependent manner (**Figure 4** and **Table 1**).

The effect of e16 on SMMC-7721 cell cycle pattern

SMMC-7721 cells were treated by R16 at a concentration of 2.543 μmol·L^{-1}, 3.912 μmol·L^{-1}, and 5.427 μmol·L^{-1}, respectively, for 24 hours. Compared with the control group, R16 treated group showed significantly increased number of cells at G_0/G_1 phase (P=0.011, 0.001, and <0.001), no significant changes of cell number at S phase (P=0.054, 0.906, and 0.683), significantly decreased number of cells at G_2/M phase (P=0.024, <0.001, and <0.001), and significantly increased number of cells at Sub-G_1 phase (P=0.031, 0.001 and <0.001). These results showed that R16 arrested SMMC-7721 cell cycle at c-S phase, and inhibited cell division and proliferation, as shown in **Figure 5.**

The effect of R16 on cellular p53 and caspase-3 expression

SMMC-7721 were treated by R16 at a concentration of 2.543 μmol·L^{-1}, 3.912 μmol·L^{-1}, and 5.427 μmol·L^{-1}, respectively, for 24 hours. p53 and caspase-3 protein expression levels were detected by Western blot. Compared with the control group, p53 expression was significantly increased following R16 treatment, in a concentration dependent manner. Caspase-3 ex-

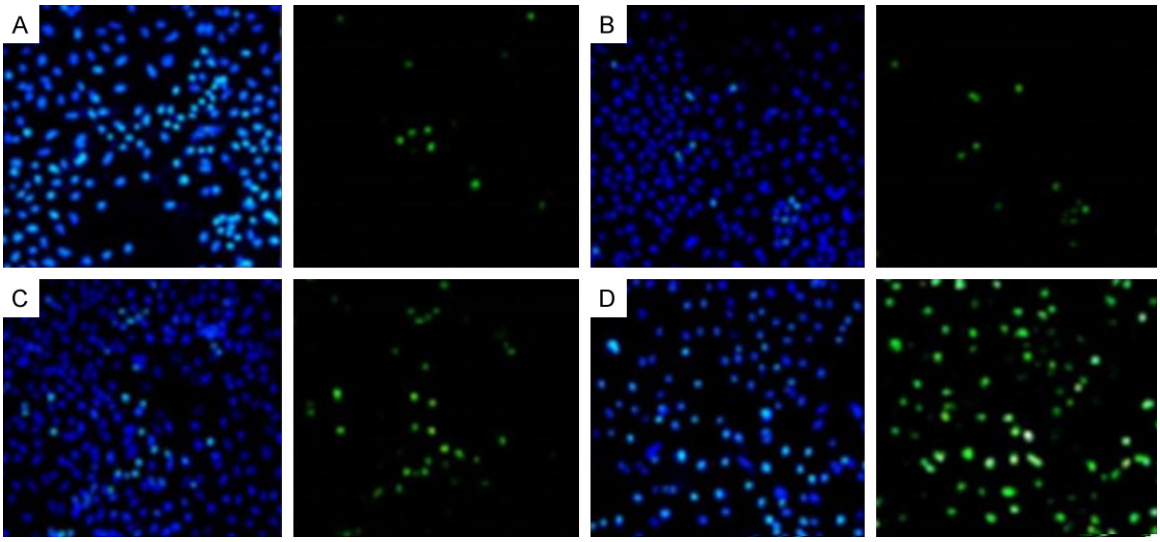

Figure 4. Induction of apoptosis of SMMC-7721 cells treated with R16 for 24 hours evaluated by TUNEL assay. Representative images were taken, nuclear stain (DAPI, Left) and apoptotic stain (TUNEL, Right) overlaid. A: Control; B: R16 (2.543 μmol·L^{-1}); C: R16 (3.912 μmol·L^{-1}); D: R16 (5.427 μmol·L^{-1}) Magnifcation, 100 ×.

Table 1. Apoptotic effects of R16 on SMMC-7721 cells ($\bar{x}$ ± s, n=3)

Group	Dose/μmol·L^{-1}	Apoptotic ratio/%
Control		4.15±4.57
R16	2.543	33.85±4.19**
	3.912	47.62±7.81**
	5.427	66.54±6.92**

**p<0.01 vs control.

pression was also increased, as well as active fragments (**Figure 6**).

Discussion

In this study, the anti-cancer unsaturated ketone skeleton of rhodanine was assembled with fluoroquinolone skeleton at the C-3 position to construct a series of target compounds of amide fluoroquinolones (rhodanine unsaturated ketone). MTT assay was used to screen the target compounds. Twelve fluoroquinolone-rhodanine derivatives had an IC_{50} below 50 μmol·L^{-1} after 24 hour treatment on human hepatocellular carcinoma cells SMMC-7721. Among these derivatives, the IC_{50} of R16 was 3.893 μmol·L^{-1}, which was significantly lower than that of the parent compound rufloxacin (226.924 μmol·L^{-1}), and also lower than that of the clinical anti-cancer agent sunitinib (7.846 μmol·L^{-1}). This results indicate that it was worthy further research and development to investigate rufloxacin-rhodanine derivatives, which were constructed by assembling rufloxacin and rhodanine unsaturated ketone skeleton, as anti-cancer agents.

In order to understand the difference of R16 on various cancer cells, three types of cancer cells lines (human hepatocellular carcinoma cells SMMC-7721, esophageal cancer cells EC-9706, and colon cancer CaCO-2 cells) were investigated in this study to detect the inhibitory effect of R16 on cell growth. The results show that R16 exhibited a significantly inhibitory effect on proliferation of various types of cancer cells. This effect was shown in a time and concentration dependent manner. In this study hepatocyte cell line L-02 was also cultured *in vitro* to detect inhibitory effect of R16 on cell growth. The IC_{50} on L-02 was 35.244 μmol·L^{-1}, significantly higher than that of R16 on SMMC-7721 cells. This suggested the selectivity of R16 on cancer cells and possibly less toxic effects in its future use in clinical practice.

The preliminary experiments of this study demonstrate that the significant anti-cancer activity of fluoroquinolone derivatives with modified C-3 carboxyl group was mainly exhibited on DNA topoisomerase II, by inhibiting the activity of DNA topoisomerase II activity and interfering with DNA replication [11, 12]. This study detected the changes of SMMC-7721 cell cycle

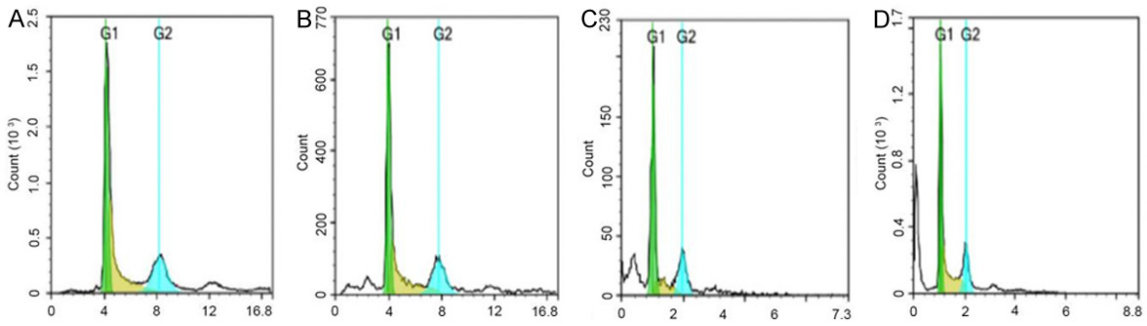

Figure 5. Effect of R16 on the cell cycle distribution in SMMC-7721 cells. Cell cycle distribution was demonstrated by Flow cytometry analysis in SMMC-7721 cells after treatment with 0 (A), 2.543 (B), 3.912 (C) and 5.427 μmol·L^{-1} (D) R16 respectively for 24 hours.

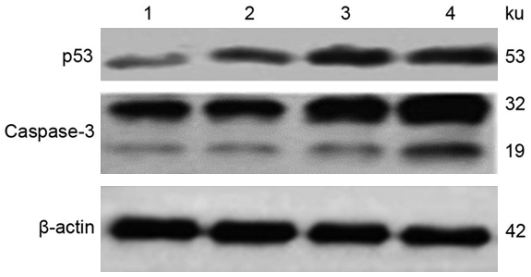

Figure 6. Effects of R16 on p53 and caspase-3 protein expression in SMMC-7721 cells. 1: Control; 2: R16 (2.543 μmol·L^{-1}); 3: R16 (3.912 μmol·L^{-1}); 4: R16 (5.427 μmol·L^{-1}).

following R16 treatment by PI staining and flow cytometry. The results show that, compared with the control group, the cell number at G_0/G_1 phase was significantly increased, accompanied by decreased cell number at G_2/M phase and no change in S phase, indicating that cell cycle was arrested at G_1-S phase. This change was associated with DNA replication. DNA topoisomerase II is able to catalyze the mutual transformation of DNA topological isomers, catalyze the disconnection and binding of DNA double strands, and promote DNA helix unwinding to complete the replication process [13]. DNA topoisomerase II toxin led to irreversible broken DNA and damage. The action may activate p53 protein and induce apoptosis [14, 15]. In our experiments, changes of p53 expression were detected by Western-blot. The results suggest that R16 killed SMMC-7721 by DNA damage, and enhanced p53 expression and induction of the apoptotic pathway. The changes in nuclear morphology in SMMC-7721 cells were observed by DAPI staining. Apoptotic SMMC-7721 cells were increased following 24 hour treatment of R16, shown by changes in nuclear morphology including nucleus shrinkage and fragmentation, chromatin condensation, marginalization, and appearance of apoptotic bodies [16]. TUNEL assay showed significantly enhanced caspase-3 expression and cleavage fragments with the increased R16 concentration. The results indicate that R16 induced apoptosis by activating capase-3 pathway.

In summary, modified rufloxacin-rhodanine derivatives arrested cell cycle at G_1-S phase, and significantly inhibited division and proliferation of cancer cells, such as hepatocellular carcinoma cells, in a selective manner. The anticancer effect of R16 was mainly accomplished by induction of apoptosis [17].

Acknowledgements

This work was supported by the National Natural Science Foundation of China (21072045) and Henan Natural Science Foundation (112102310307).

Disclosure of conflict of interest

None.

Address correspondence to: Bin Liu, Institute of Nursing and Health, Henan University, Jin Ming Avenue, College of Nursing and Health, Kaifeng 475004, China. Tel: +86- 371-23880399; Fax: +86-371-23880399; E-mail: byx0552@163.com

References

[1] Singh S, Kaur G, Mangla V and Gupta MK. Quinoline and quinolones: promising scaffolds for future antimycobacterial agents. J Enzyme Inhib Med Chem 2015; 30: 492-504.

[2] Patel MN, Bhatt BS and Dosi PA. Topoisomerase inhibition, nucleolytic and electrolytic contribution on DNA binding activity exerted by biological active analogue of coordination compounds. Appl Biochem Biotechnol 2012; 166: 1949-1968.
[3] Schmidt BH, Osheroff N and Berger JM. Structure of a topoisomerase II-DNA-nucleotide complex reveals a new control mechanism for ATPase activity. Nat Struct Mol Biol 2012; 19: 1147-1154.
[4] Berger JM, Gamblin SJ, Harrison SC and Wang JC. Structure and mechanism of DNA topoisomerase II. Nature 1996; 379: 225-232.
[5] Williams GM, Brunnemann KD, Smart DJ, Molina D, Jeffrey AM, Duan JD, Krebsfaenger N, Kampkoetter A and Schmuck G. Relationship of cellular topoisomerase IIα inhibition to cytotoxicity and published genotoxicity of fluoroquinolone antibiotics in V79 cells. Chem Biol Interact 2013; 203: 386-390.
[6] Jiang M, Huang O, Xie Z, Wu S, Zhang X, Shen A, Liu H, Chen X, Wu J, Lou Y, Mao Y, Sun K, Hu S, Geng M and Shen K. A novel long non-coding RNA-ARA: adriamycin resistance-associated. Biochem Pharmacol 2014; 87: 254-283.
[7] Wang Z, Liang S, Lian X, Liu L, Zhao S, Xuan Q, Guo L, Liu H, Yang Y, Dong T, Liu Y, Liu Z and Zhang Q. Identification of proteins responsible for adriamycin resistance in breast cancer cells using proteomics analysis. Sci Rep 2015; 5: 9301.
[8] Ahmed A and Daneshtalab M. Nonclassical biological activities of quinolone derivatives. J Pharm Pharm Sci 2012; 15: 52-72.
[9] Liang JH and Han X. Structure-activity relationships and mechanism of action of macrolides derived from erythromycin as antibacterial agents. Curr Top Med Chem 2013; 13: 3131-3164.
[10] Bringmann G, Dreyer M, Faber JH, Dalsgaard PW, Staerk D, Jaroszewski JW, Ndangalasi H, Mbago F, Brun R and Christensen SB. Ancistrotanzanine C and related 5,1'- and 7,3'-coupled naphthylisoquinoline alkaloids from Ancistrocladus tanzaniensis. J Nat Prod 2004; 67: 743-748.
[11] Sun JP, Shi ZY, Liu SM, Kang YH, Hu GQ, Huangfu CS, Deng JB and Liu B. Trimethoxy-benzaldehyde levofloxacin hydrazone inducing the growth arrest and apoptosis of human hepatocarcinoma cells. Cancer Cell Int 2013; 13: 67.
[12] Huo F, Tang NF, Fan YY, Liu SM, Zhang Y, Hu GQ and Liu B. Benzaldehyde levofloxacin schiff base induces apoptosis of human hepatocarcinoma cells. Chinese Pharmacological Bulletin 2015; 31: 821-826.
[13] Orlowski C, Mah LJ, Vasireddy RS, El-Osta A and Karagiannis TC. Double-strand breaks and the concept of short- and long-term epigenetic memory. Chromosoma 2011; 120: 129-149.
[14] Wanitchakool P, Jariyawat S, Suksen K, Soorukram D, Tuchinda P and Piyachaturawat P. Cleistanthoside A tetraacetate-induced DNA damage leading to cell cycle arrest and apoptosis with the involvement of p53 in lung cancer cells. Eur J Pharmacol 2012; 696: 35-42.
[15] Calviño E, Estañ MC, Simón GP, Sancho P, Boyano-Adánez Mdel C, de Blas E, Bréard J and Aller P. Increased apoptotic efficacy of lonidamine plus arsenic trioxide combination in human leukemia cells. Reactive oxygen species generation and defensive protein kinase (MEK/ERK, Akt/mTOR) modulation. Biochem Pharmacol 2011; 82: 1619-1629.
[16] Omlor GW, Nerlich AG, Tirlapur UK, Urban JP and Guehring T. Loss of notochordal cell phenotype in 3D-cell cultures: implications for disc physiology and discrepair. Arch Orthop Trauma Surg 2014; 134: 1673-1681.
[17] Liese J B, Abhari A and Fulda S. Smac mimetic and oleanolic acid synergize to induce cell death in human hepatocellular carcinoma cells. Cancer Lett 2015; 365: 47-56.